

# Total electron content monitoring using triple frequency GNSS: Results with Giove-A/-B data

J. Spits\*, R. Warnant

Royal Meteorological Institute, Avenue Circulaire 3, 1180 Brussels, Belgium

Received 26 February 2010; received in revised form 30 June 2010; accepted 21 August 2010

## Abstract

Triple frequency GNSS will be fully operational within the next decade, opening opportunities for new applications. Dual frequency GNSS already allow to study the ionosphere through the estimation of Total Electron Content (TEC). However, the precision is limited by the ambiguity resolution process. This paper studies a triple frequency TEC monitoring technique in which the use of Geometry-Free and Iono-Free linear combinations improves the ambiguity resolution process and therefore the precision of TEC. We have tested it on a set of triple frequency Giove-A/-B data from January and December 2008. The conclusions achieved are (1) TEC values are affected by an error of about 2–2.5 TECU produced through the ambiguity resolution process; (2) the error caused by the Geometric Free phase combination delays (hardware, multipath, noise, antenna phase center) on TEC is about 0.2 TECU; (3) the total error on TEC approximately reach 2–3 TECU.

© 2010 COSPAR. Published by Elsevier Ltd. All rights reserved.

**Keywords:** Ionosphere; TEC; GNSS; Triple frequency

## 1. Introduction

Triple frequency Global Navigation Satellite Systems (GNSS) will be fully operational within the next decade. Nowadays, the Global Positioning System (GPS) transmits two carrier signals, while the third frequency (Table 1) is under commissioning. Galileo transmits in three frequency bands (L1–E5–E6) whereby for E5 we will have the choice of three signals (E5a, E5b and E5-AltBOC, see Table 1). The open services are realized by using the L1 and E5 signals, while E6 signals are encrypted. Up to now, the first two Galileo test satellites, Giove-A and Giove-B, have been launched and tested successfully.

Dual frequency GNSS measurements makes it possible to reconstruct the slant total electron content (TEC) of the ionosphere, i.e. the integral of the electron concentration on the receiver-to-satellite path. TEC is computed by

using Geometric Free (GF) combinations of one-way code ( $P_{p,k}^i$ ) and/or phase ( $\Phi_{p,k}^i$ ) measurements, respectively, in meters and cycles:

$$P_{p,GF}^i = P_{p,k}^i - P_{p,m}^i \quad (1)$$

$$\Phi_{p,GF}^i = \Phi_{p,k}^i - (f_k/f_m)\Phi_{p,m}^i \quad (2)$$

with  $f$  the frequency and  $k, m$  the carrier considered.

In that combination, all frequency-independent effects are eliminated, so that only ionospheric delay and other frequency-dependent effects remain, such as satellite and receiver hardware delays, multipath delays, measurement noise, satellite and receiver antenna phase center delays and – for phase measurements – the integer ambiguity  $N_{p,k}^i$ . While neglecting multipath delays, measurement noise and hardware/antenna phase delays, Eqs. (1) and (2) can be rewritten in function of TEC (expressed in TECU, with 1 TECU being  $10^{16}$  electrons/m<sup>2</sup>):

$$P_{p,GF}^i = b_{km} \text{TEC}_{km} + \text{DCB}_p^i \quad (3)$$

$$\Phi_{p,GF}^i = a_{km} \text{TEC}_{km} + N_{p,GF}^i \quad (4)$$

\* Corresponding author. Tel.: +32 2 373 67 29; fax: +32 2 374 67 88.  
E-mail addresses: [Justine.Spits@oma.be](mailto:Justine.Spits@oma.be) (J. Spits), [R.Warnant@oma.be](mailto:R.Warnant@oma.be) (R. Warnant).

Table 1  
GPS and Galileo frequencies and wavelengths.

GNSS	Carrier signal	Frequency (MHz)	$\lambda$ (m)
GPS	L1	1575.42	0.1903
	L2	1227.60	0.2442
	L5	1176.45	0.2548
Galileo	L1	1575.42	0.1903
	E6	1278.42	0.2345
	E5b	1207.14	0.2483
	E5a + b	1191.795	0.2515
	E5a	1176.45	0.2548

with

$$a_{km} = 40.3 \times 10^{16} (f_k/c) (1/f_m^2 - 1/f_k^2)$$

$$b_{km} = 40.3 \times 10^{16} (1/f_k^2 - 1/f_m^2)$$

As phase measurements are much less affected by measurement noise and multipath delays than code measurements (Manucci et al., 1998), TEC is computed from the GF phase combination  $\Phi_{p,GF}^i$ . The main issue in Eq. (4) is the resolution of the so-called real GF ambiguity  $N_{p,GF}^i$  (in cycles):

$$N_{p,GF}^i = N_{p,k}^i - (f_k/f_m) N_{p,m}^i \quad (5)$$

When using GPS or GLONASS dual frequency L1/L2 measurements, this is usually done by the phase-to-code levelling process, which consists in shifting the GF phase combination  $\Phi_{p,GF}^i$  by a constant value ( $N_{p,GF}^i$ ) to match the GF code combination  $P_{p,GF}^i$ . It requires the computation of differential satellite and receiver code hardware delays ( $DCB_p^i$ ), which are then injected in Eq. (6) to solve the GF ambiguity.

$$P_{p,GF}^i - \lambda_k \Phi_{p,GF}^i = DCB_p^i - \lambda_k N_{p,GF}^i \quad (6)$$

According to Ciruolo et al. (2007), there remains a levelling error from 1 to 5 TECU in the GF ambiguity, due to code multipath delays but also to variations in  $DCB_p^i$ . This constitutes the main limit to TEC reconstruction using dual frequency measurements (Brunini and Azpilicueta, 2009; Ciruolo et al., 2007; Warnant and Pottiaux, 2000).

With triple frequency GNSS – modernized GPS and Galileo – other linear combinations of measurements are available. This opens opportunities for new applications, e.g. improved multipath mitigation and multi-frequency ambiguity resolution algorithms (Simsky, 2006). This paper presents a triple frequency TEC monitoring technique in which the use of linear combinations, and in particular Geometry-Free and Iono-Free combinations, improves the ambiguity resolution process and therefore the precision of TEC.

We will first explain the methodology developed for triple frequency data (Section 2), and then present the results obtained with a set of L1–E5b–E5a Giove-A/-B data (Section 3). This corresponds to the open services, while E6 signals are encrypted (Table 1). For more readability in the equations, which can also be applied to GPS, the E5a channel which has the same frequency as L5 will be named L5,

and the E5b channel will be named L2 for convenience. However the reader should be warned that the frequencies for GPS L2 and Galileo E5b are not the same and that the coefficients in the linear combinations therefore also have different values. In the context of this paper L2 should simply be considered as the second frequency.

## 2. Methodology

Our methodology is divided in four main steps. The first three steps aim at ambiguity resolution in order to be able to compute TEC in the fourth one.

### 2.1. Extra-widelane ambiguity resolution

The objective of this step is to resolve extra-widelane (EWL) ambiguities  $N_{25}$  by using the extra-widelane-narrowlane (EWLNL) combination  $C_{25}$  (in cycles):

$$C_{25} = \Phi_{p,L2}^i - \Phi_{p,L5}^i - \frac{f_{L2} - f_{L5}}{f_{L2} + f_{L5}} \times \left( \frac{f_{L2}}{c} P_{p,L2}^i + \frac{f_{L5}}{c} P_{p,L5}^i \right)$$

$$= N_{p,L5}^i - N_{p,L2}^i + \Delta C_{25} = N_{25} + \Delta C_{25} \quad (7)$$

This is actually the Melbourne–Wübbena combination (Melbourne, 1985; Wübbena, 1985) applied to L2 and L5 frequencies and expressed in meters. This combination is Geometry-Free and Iono-Free and gives the integer ambiguities  $N_{25}$  plus a residual term  $\Delta C_{25}$  depending on hardware delays, multipath delays and measurement noise on both code and phase measurements.

The wavelength of  $C_{25}$  is significantly increased and equals 9.768 m for Galileo, which makes the resolution of integer ambiguities easier. In this case, it is critical that the residual term  $\Delta C_{25}$  be less than half a extra-widelane wavelength (0.5 cycle or 4.884 m) to resolve EWL ambiguities, which leaves room for other errors.

To assess the influence of  $\Delta C_{25}$ , we first consider multipath delays and measurement noise as quasi random errors. By using the values of standard deviations (SD) given in Table 2, the law of error propagation gives us a SD on  $C_{25}$  equals to 0.027 cycles. Secondly, because of the lack of information about hardware delays, we have to make several assumptions: we consider that satellite and receiver code and phase hardware delays – which are usually constant in time (Brunini and Azpilicueta, 2009) – follow a normal distribution with  $\mu = 0$  and with 99% of

Table 2

Standard deviation of code/phase measurement noise and multipath delays for Galileo observables (Simsky and Sleewagen, 2005; Simsky et al., 2006, 2008).

	Signal	Noise SD (m)	Multipath SD (m)
Code	L1	0.18	0.4
	E5b	0.11	0.2
	E5a	0.11	0.2
Phase	L1	0.0019	0.003
	E5b	0.0024	0.003
	E5a	0.0025	0.003

values below 3 m and 1 mm, respectively, for code and phase delays. On that basis we find a SD on  $C_{25}$  equal to 0.084 cycle (either satellite or receiver). By addition of all errors, we finally obtain a SD of 0.122 cycle. Considering a 99% level of confidence (2.58 SD), the error on  $C_{25}$  will not be greater than 0.31 cycle, which means that the  $C_{25}$  combination can be used to resolve EWL ambiguities.

## 2.2. Widelane ambiguity resolution

The objective of the second step is to resolve the integer widelane (WL) ambiguities  $N_{12}$  by forming the so-called widelane-narrowlane (WLNL) combination  $C_{12}$  (in cycles):

$$\begin{aligned} C_{12} &= \Phi_{p,L1}^i - \Phi_{p,L2}^i - \frac{f_{L1} - f_{L2}}{f_{L1} + f_{L2}} \times \left( \frac{f_{L1}}{c} P_{p,L1}^i + \frac{f_{L2}}{c} P_{p,L2}^i \right) \\ &= N_{p,L2}^i - N_{p,L1}^i + \Delta C_{12} = N_{12} + \Delta C_{12} \end{aligned} \quad (8)$$

Similarly to  $C_{25}$ , this combination – the Melbourne–Wübbena combination (Melbourne, 1985; Wübbena, 1985) – is Geometry-Free and Iono-Free and gives the integer ambiguities  $N_{12}$  plus a residual term  $\Delta C_{12}$  depending on hardware delays, multipath delays and measurement noise on both code and phase measurements.

The wavelength of  $C_{12}$  – using L1 and E5b – equals 0.814 m for Galileo (for GPS – using L1 and L2 – this is 0.862 m), which is 12 times smaller than the EWLNL combination wavelength. Following the same procedure than in Section 2.1, the total SD on  $C_{12}$  equals 1.478 cycle (multipath and noise: 0.33 cycle – hardware delays: 1.44 cycles), which leads to a total error of 3.81 cycles. As a consequence  $C_{12}$  combination does not allow to resolve WL ambiguities.

We tried to resolve WL ambiguities with another combination called differenced widelane (DWL) combination  $C_{125}$  (in cycles):

$$\begin{aligned} C_{125} &= \left( \Phi_{p,L1}^i - \Phi_{p,L2}^i \right) - \left( \Phi_{p,L2}^i - \Phi_{p,L5}^i - N_{25} \right) \frac{\lambda_{25}}{\lambda_{12}} \\ &= N_{p,L2}^i - N_{p,L1}^i + \Delta C_{125} = N_{12} + \Delta C_{125} \end{aligned} \quad (9)$$

This combination is Geometry-Free but not Iono-Free; it gives the integer ambiguities  $N_{12}$  plus a residual term  $\Delta C_{125}$  depending on all phase delays but also on the ionosphere by a contribution – in cycles – of  $0.08 \times \text{TEC}$  (with TEC being in TECU). Even without taking the influence of phase delays into account,  $\Delta C_{125}$  can clearly exceed 0.5 cycle (Spits and Warnant, 2008).

In other words, neither  $C_{12}$  nor  $C_{125}$  makes the resolution of  $N_{12}$  possible. Those WLNL and DWL combinations only give approximated integer values of the WL ambiguities.

## 2.3. Final ambiguity resolution

The objective of this step is to resolve the integer ambiguities  $N_1, N_2, N_5$ . For this purpose, we use a Geometry-

Free and Iono-Free triple frequency phase combination  $s_{125}$  (Simsy, 2006), expressed here in meters:

$$\begin{aligned} s_{125} &= a_1 \lambda_1 \Phi_{p,L1}^i + a_2 \lambda_2 \Phi_{p,L2}^i + a_5 \lambda_5 \Phi_{p,L5}^i \\ &= -a_1 \lambda_1 N_1 - a_2 \lambda_2 N_2 - a_5 \lambda_5 N_5 + \Delta s_{125} \end{aligned} \quad (10)$$

Each  $a_i$  coefficient is unitless and depends on a combination of  $\lambda_i$ , with  $a_1 \approx 0.128$ ,  $a_2 \approx -1.128$  and  $a_5 = 1$  for Galileo L1, E5b and E5a. The  $s_{125}$  combination only depends on the ambiguities and on phase delays (hardware, multipath, noise and antenna phase center) which form the residual term  $\Delta s_{125}$ . By averaging  $s_{125}$  on a whole satellite pass without cycle slip ( $\overline{s_{125}}$ ), we can consider phase multipath delays and phase measurement noise as negligible, so that the residual term  $\Delta \overline{s_{125}}$  is only function of phase hardware delays and residual antenna phase center delays. Note that if we do not average  $s_{125}$ , it would lead to a – nearly one order of magnitude – bigger error.

If we introduce  $N_{25}$  and  $N_{12}$  from previous steps, we can obtain  $N_2$  (and so  $N_1, N_5$ ) as follows:

$$N_2 = \frac{\overline{s_{125}} - a_1 \lambda_1 N_{12} + a_5 \lambda_5 N_{25} - \Delta \overline{s_{125}}}{-(a_1 \lambda_1 + a_2 \lambda_2 + a_5 \lambda_5)} \quad (11)$$

We neglect the residual term in a first step. We know from Section 2.2 that  $N_{12}$  are only approximated integer values, so are the  $N_2$  resulting values. As in Eq. (11) an error of +1 cycle on  $N_{12}$  corresponds to an error of –25.55 cycles on  $N_2$  and consequently to an error of respectively –25.55 and –26.55 cycles for  $N_5$  and  $N_1$ , we can derive from Eqs. (4) and (5) that this leads to an error of +11.327 TECU on TEC. On this basis, the use of approximated TEC values computed by the classical dual frequency method allows us to fix  $N_{12}$  at their correct integer values. This can be achieved by following the procedure presented in Spits and Warnant (2008), i.e.

1. We introduce the approximated values of  $N_{12}$  obtained from Eq. (8) or Eq. (9) in Eq. (11) in order to compute the approximated values of  $N_2$ , and then derive  $N_5$  and  $N_1$ , respectively, from  $N_{25}$  and  $N_{12}$ .
2. We introduce the approximated values of  $N_1, N_2$  and  $N_5$  in Eq. (5), so that we obtain the approximated TEC values called  $\text{TEC}_a$  (the correct ones are referred to as  $\text{TEC}_b$ ).
3. We compute approximated TEC values  $\text{TEC}_e$  by leveling dual frequency phase measurements with Global Ionospheric Maps or GIM (Feltens and Schaer, 1998), following the method described in Orus et al. (2007) and in Bidaine and Warnant (2009).
4. We compute  $\Delta \text{TEC}_e = \text{TEC}_a - \text{TEC}_e$ , i.e. the difference between the approximated and estimated values of TEC, which gives an approximation of  $\Delta \text{TEC}_b = \text{TEC}_a - \text{TEC}_b$ , i.e. the real error made on TEC values.
5. Using the property mentioned above, we are now able to compute  $\Delta N_{12-e} = \Delta \text{TEC}_e / 11.327$  which gives an approximation of the real error made on the WL ambiguities ( $\Delta N_{12-b} = \Delta \text{TEC}_b / 11.5$ ). This approximation

will be precise enough to correctly resolve  $N_{12}$  if  $\Delta\text{TEC}_e$  is more accurate than half of 11.327 TECU, so approximately 5–6 TECU. The accuracy of  $\Delta\text{TEC}_e$  depends on the errors in  $\text{TEC}_a$  – caused by the residual term  $\Delta\overline{s_{125}}$  in the ambiguity resolution plus by phase delays in the GF phase combination (Section 2.4) – as well as on the errors inherent in  $\text{TEC}_e$ , corresponding to the uncertainty of GIMs. As stated later, the former should not exceed 2–3 TECU; the latter depend on the mean global TEC, with worse performance at low latitude and in period of high solar activity. However it might not be the case in daytime equatorial conditions, we can make the assumption that the accuracy of  $\Delta\text{TEC}_e$  will be better than 5–6 TECU.

6. We introduce the correct values of  $N_{12}$  in Eq. (11), so that we finally obtain the correct values of  $N_2$  and therefore of  $N_5$  and  $N_1$ .

What is now the influence of the residual term  $\Delta\overline{s_{125}}$ ? According to the theoretical values given in Section 2.1, the SD on  $\overline{s_{125}}$  due to hardware delays equals  $8.29 \times 10^{-4}$  m, which by Eq. (11) makes 0.869 cycles on  $N_2$ . With a 99% level of confidence, it could lead to an error of 2.2 cycles (round up to 2) on  $N_2$ ,  $N_1$  and  $N_5$ . As they are elevation-dependent, the effects of antenna phase center delays in  $\overline{s_{125}}$  are averaged, so that we will assume that the error budget is multiplied by a factor 2, i.e. 4.4 cycles on the ambiguities. Finally, Eqs. (4) and (5) show that the resulting error on TEC would reach about 2–2.5 TECU. As it is related to errors on the ambiguities – which are integer numbers – this cannot be considered as a random error: each error of 1 cycle induces an error of about 0.5 TECU.

#### 2.4. TEC computation

The objective of this step is to compute TEC. As in previous steps we have resolved all integer ambiguities ( $N_1, N_2, N_5$ ), we can introduce them in Eq. (5) to resolve  $N_{p,GF}^i$  and then to compute TEC by using Eq. (4). TEC can be obtained from three different GF combinations: L1/L2, L1/L5 and L2/L5; we shall refer to these different TEC values as  $\text{TEC}_{12}$ ,  $\text{TEC}_{15}$  and  $\text{TEC}_{25}$ .

To assess the influence of all phase delays on TEC, which are neglected in Eq. (4), let us first have a look to  $a_{km}$  coefficients ( $a_{12} = 0.600$ ,  $a_{15} = 0.676$  and  $a_{25} = 0.058$ ). As  $a_{25}$  is one order of magnitude smaller than the two other coefficients, and as phase delays have approximately the same amplitude on all frequencies (Table 2), we can already conclude that  $\text{TEC}_{25}$  will be less precise. Following the law of error propagation (Section 2.1), the SD on TEC due to multipath, noise and hardware delays equals 0.046, 0.041 and 0.382 TECU, respectively, for  $\text{TEC}_{12}$ ,  $\text{TEC}_{15}$  and  $\text{TEC}_{25}$ . The total error caused by those phase delays is then given by 2.58 SD and equals 0.120, 0.107 and 0.987 TECU. Even if there is no average effect here, we can still consider that the influence of antenna phase center delays will mul-

tiple the error budget by a factor 2, reaching about 0.2 TECU for  $\text{TEC}_{12}$  and  $\text{TEC}_{15}$ . From all this, it follows that the best way to estimate TEC is to have the frequencies as far apart as possible. In other words, we will not compute TEC using L2/L5.

Finally, taking into account the error caused by the ambiguity resolution (Section 2.3) together with the one caused by phase delays, the total error on TEC ( $\text{TEC}_{12}$  or  $\text{TEC}_{15}$ ) would reach about approximately 2–3 TECU.

### 3. Results

This section provides the results obtained with a set of triple frequency L1–E5b–E5a Giove-A/-B data, presented in Table 3. Note that for GIEN, GKOU and GNOR we only have Giove-A data, as for GMIZ only Giove-B data.

Fig. 1 shows the EWLNL combination  $C_{25}$  in four cases (one per station). The variability of this combination is about 0.02 cycle. By computing the SD of  $C_{25}$  for the whole data set (representing the variable part of it, i.e. noise and multipath), we find values in agreement with the theoretical values obtained in Section 2.1, i.e. 0.027 cycle. Furthermore, as we can mathematically demonstrate that an error on  $N_{25}$  would have caused a huge error on TEC values, we can confirm the statements of Section 2.1, i.e. that we are able to fix EWL ambiguities at their correct integer values.

Fig. 2 respectively shows the WLNL combination  $C_{12}$  and the DWL combination  $C_{125}$  for two satellite passes, a Giove-A pass in GNOR station and a Giove-B pass in GMIZ station. First, the SD of  $C_{12}$  is about 0.3 cycle for the whole data set, which is in agreement with the theoretical values derived in Section 2.2, i.e. 0.33 cycle. Then, we can observe that the variability of  $C_{125}$  – due to ionosphere, multipath and noise – is relatively large (around 0.25 cycle). In both cases, even without taking hardware delays (that act as a bias) into account, the resolution of  $N_{12}$  is impossible. As already said in Section 2.2, we only obtain approximate integer values of the WL ambiguities.

However, we can see in Fig. 2 (see labels) that  $C_{12}$  and  $C_{125}$  give quite different approximated values of  $N_{12}$ , as they actually differ one from the other of approximately 190 cycles. How to explain such a difference? As code measurements are used to compute  $C_{12}$  but not  $C_{125}$ , let us first have a more detailed look at them, e.g. by computing the GF code combinations  $P_{GF12}$ ,  $P_{GF15}$ ,  $P_{GF25}$  based on Eq.

Table 3

Giove-A/-B data set. All those stations belong to the Galileo Experimental Sensor Stations Network (ESA & GSA, 2008). As Giove-A and Giove-B satellites can only transmit two frequency bands at a time (L1 + E5 or L1 + E6), we choose a L1 + E5 period. In this work, we used code and phase measurements on L1, E5b, E5a frequencies.

Station	Location	DoY 2008
GIEN	Torino, Italy	013,016,017,020
GKOU	Kourou, French Guyana	014,015,018
GNOR	Noordwijk, Netherlands	013,016,017,019,020
GMIZ	Mizusawa, Japan	337,338,341,344,345

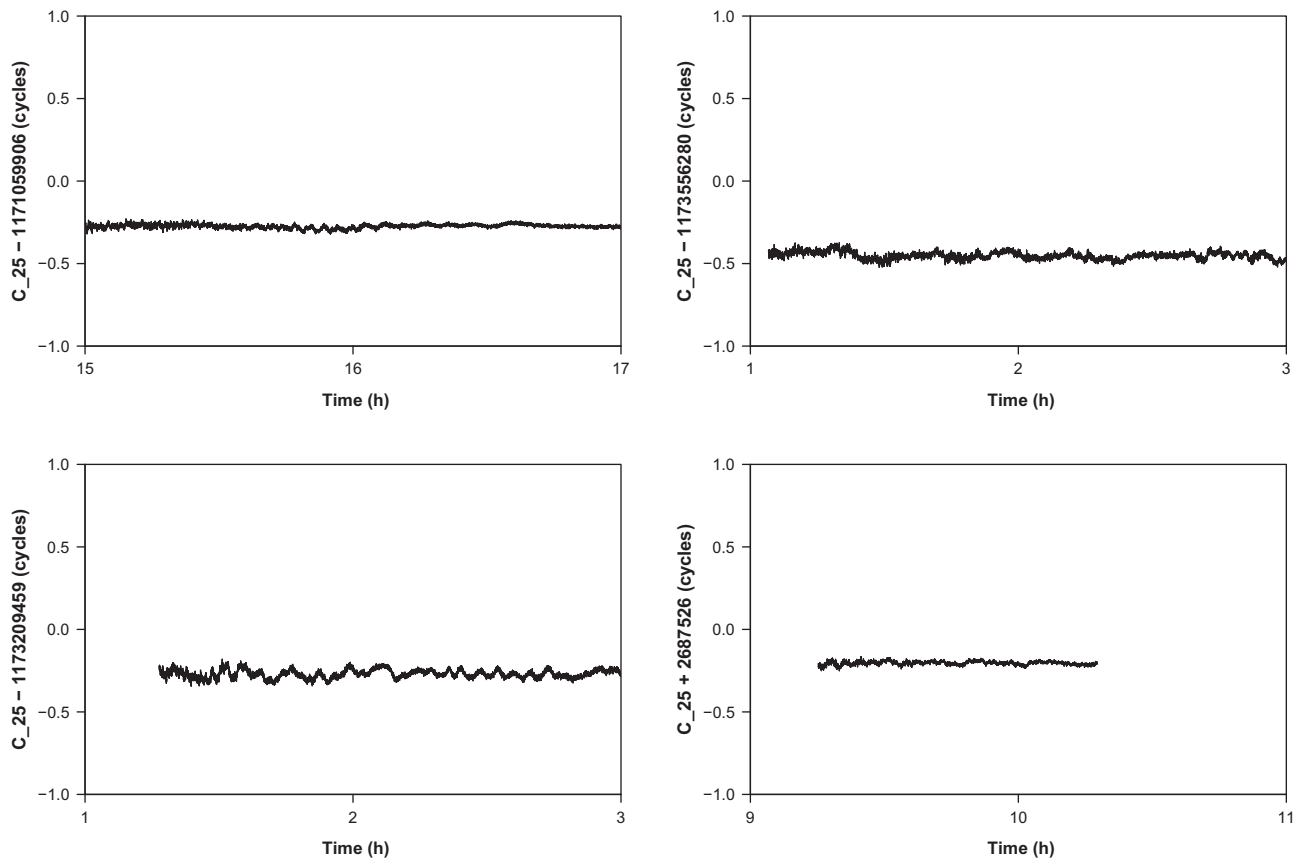


Fig. 1. EWLNL combination  $C_{25}$ , respectively – from top left to right bottom – for GIEN DoY 016/08, GKOU DoY 015/08, GNOR DoY 013/08, GMIZ DoY 338/08. For more readability, we have removed the nearest integer part of  $C_{25}$  (see labels).

(1). Those combinations actually contain all frequency-dependent delay differences, i.e. ionospheric delays plus the same code delays as in  $C_{12}$  (hardware, multipath, measurement noise). Fig. 3 shows an example of the GF code combinations for GMIZ DoY 341/08. We can see that  $P_{GF12}$  and  $P_{GF15}$  vary around 270 m, whereas  $P_{GF25}$  varies around 0 m. Similar values are observed for other days and stations, either for Giove-A or Giove-B. Which effect(s) could explain those values? If we consider for example a TEC of about 10 TECU, the difference between ionospheric delays contained in the GF code combination does not exceed 1 m for  $P_{GF12}$  or  $P_{GF15}$  and 0.1 m for  $P_{GF25}$ . This means that ionospheric delays cannot explain the magnitude (and their difference) of the different  $P_{p,GF}^i$  values observed. Moreover, regarding to their amplitude (Table 2), code multipath delays and code measurement noise could neither explain it. As  $P_{GF12} \approx P_{GF15}$  and as  $P_{GF25}$  is close to zero, it means that L2 and L5 code hardware delays are rather equal, while different from L1 ones. Considering that  $N_{25}$  are correctly resolved (see above), L2 and L5 delays should be rather small, while L1 ones rather large. As a consequence, using approximated integer values of  $N_{12}$  coming from  $C_{12}$  (and thus using code measurements on L1) gives non realistic values of  $TEC_a$ , while using approximated integer values of  $N_{12}$  coming from  $C_{125}$  (and thus using only phase measurements) do give

realistic values of  $TEC_a$ . In conclusion, as  $C_{125}$  gives a much better approximation of  $N_{12}$  values, we will prefer it to  $C_{12}$  in our computations. Moreover, as we are in a low solar activity period, we assume that  $\Delta TEC_e$  is precise enough to correctly resolve  $N_{12}$  (Section 2.3).

Fig. 4 makes the comparison between  $TEC_{12}$ ,  $TEC_{15}$  and  $TEC_{25}$  for the same period and receiver (GNOR DoY 013/08). As predicted in Section 2.4,  $TEC_{25}$  is much less precise, while  $TEC_{12}$  and  $TEC_{15}$  have the same level of precision (and cannot clearly be distinguished on the graph). In the next two figures, we will only consider  $TEC_{12}$  values.

Fig. 5 shows TEC values computed for five different days in Noordwijk and in Mizusawa. In both periods – respectively January and December 2008 – we obtain relatively low TEC values, which can be explained by the low solar activity. In each station, the day-to-day variations are due to differences in local time and in satellite position which determines the position of the ionospheric piercing point.

Fig. 6 shows differences between ‘triple frequency’ (3f) TEC values obtained by the method described here, and approximated ‘dual frequency’ (2f) TEC values obtained by levelling dual frequency phase measurements with Global Ionospheric Maps (Section 2.3). As the only difference between the methods is the way to compute the

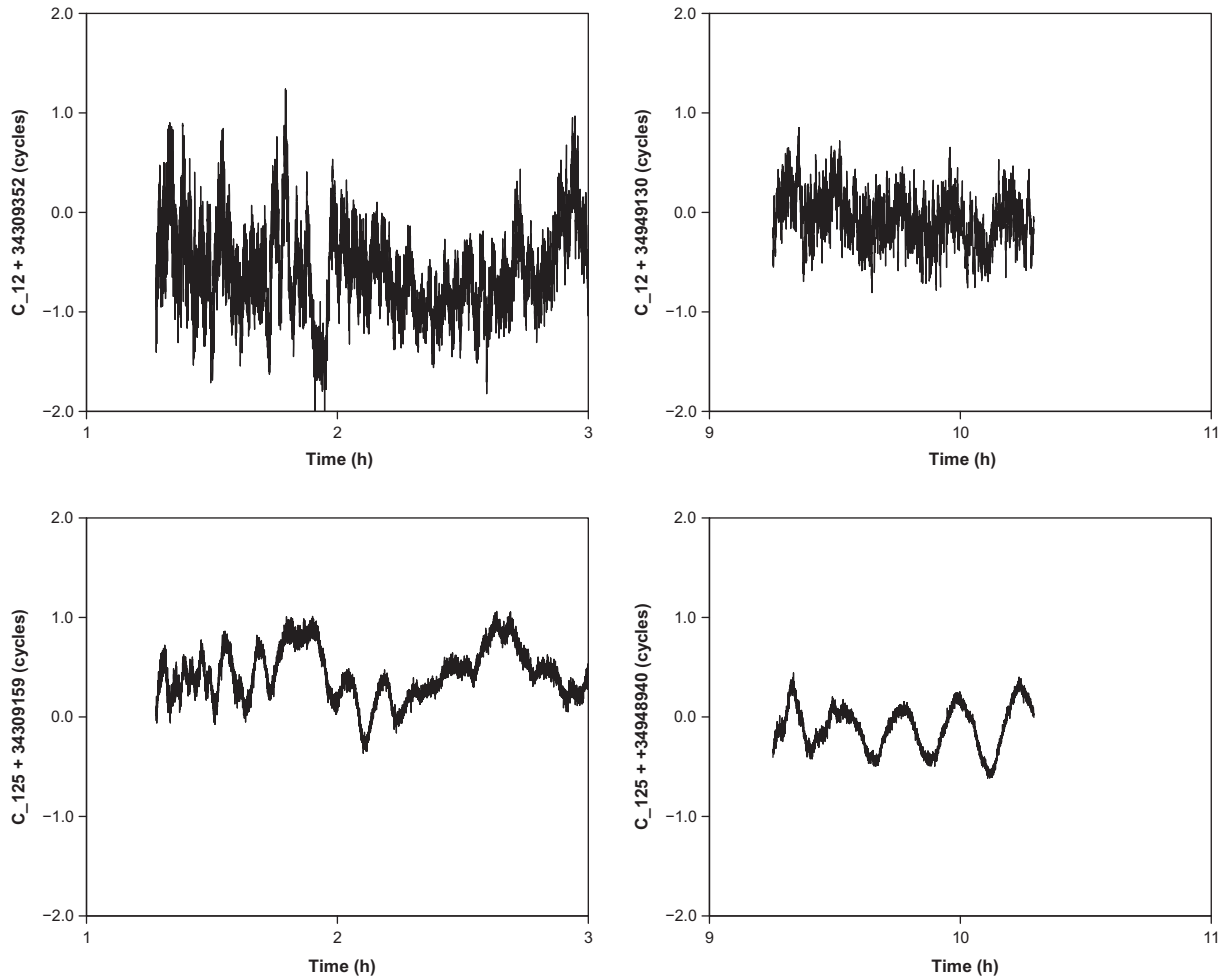


Fig. 2. WLNL combination  $C_{12}$  (top) et DWL combination  $C_{125}$  (bottom) for GNOR DoY 013/08 (left) et GMIZ DoY 338/08 (right). For more readability, we have removed the nearest integer part of  $C_{12}$  and  $C_{125}$  (see labels).

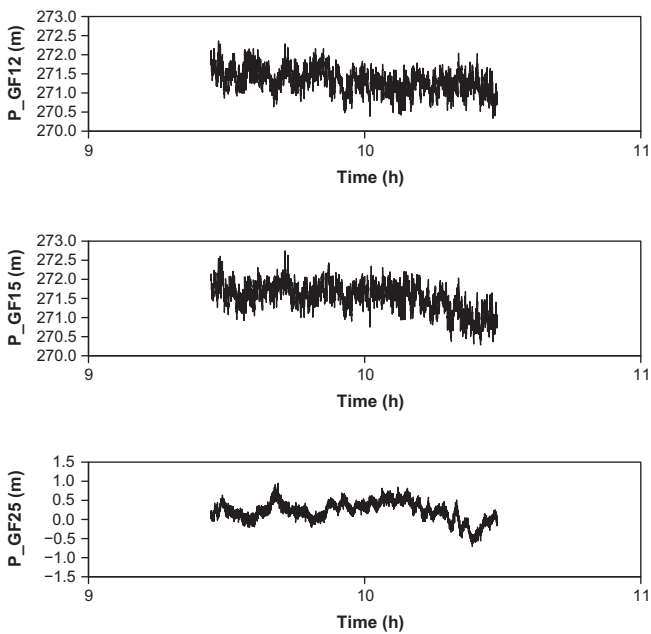


Fig. 3. GF code combinations  $P_{GF12}$  (top),  $P_{GF15}$  (middle) and  $P_{GF25}$  (bottom) for GMIZ DoY 341/08.

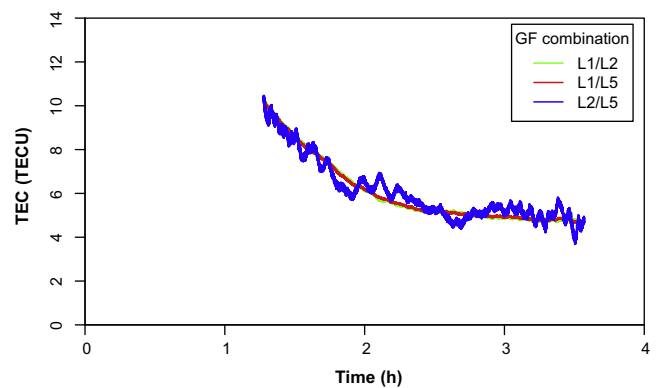


Fig. 4. TEC values for GNOR DoY 013/08 –  $TEC_{25}$  is less precise than  $TEC_{12}/TEC_{15}$ .

GF ambiguity  $N_{p,GF}^i$ , those differences are constant on each satellite pass. The magnitude of the TEC differences can be explained as follows: the 2f GF ambiguities are fixed by using interpolated TEC values of which the precision is of the order of several TECU (Orus et al., 2002), when the error budget on 3f ambiguity resolution

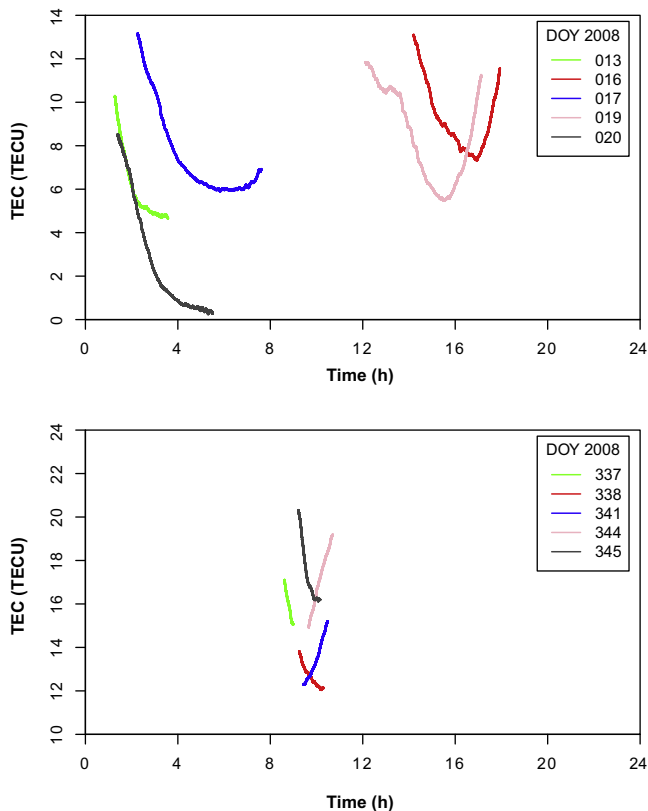


Fig. 5. TEC values obtained for Noordwijk (top) and Mizusawa stations (bottom).

as estimated in Section 2 is of the order of 2–3 TECU. Unfortunately, as the 2f method is less precise than the 3f method, this comparison does not allow to validate our results.

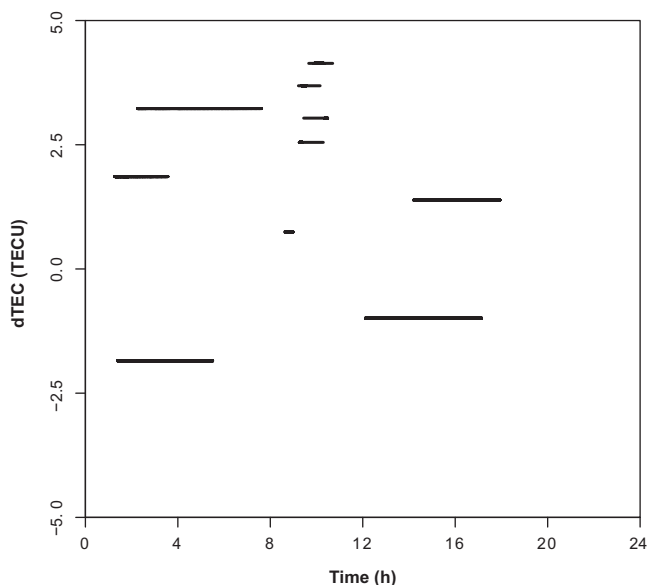


Fig. 6. Differences between 'triple frequency' TEC values and 'dual frequency' TEC values for both Noordwijk and Mizusawa stations.

#### 4. Conclusions

This paper presents an improved triple frequency TEC monitoring technique which is divided in four main steps. In the first step, the EWLNL combination  $C_{25}$  is used to resolve EWL ambiguities  $N_{25}$ . By theoretically assessing the influence of hardware delays, multipath delays and measurement noise, we conclude that it would not exceed 0.31 cycle. The results using Giove-A/B – whereby instead of GPS L2 the Galileo E5b is used – confirm the variability (i.e. influence of multipath delays and measurement noise) of  $C_{25}$ . Moreover, we can demonstrate that  $N_{25}$  are correctly resolved. In the second step, we form the WLNL  $C_{12}$  and DWL  $C_{125}$  combinations in order to resolve WL ambiguities  $N_{12}$ . In both cases, the influence of the residual term definitely exceeds 0.5 cycle, so that we only obtain approximated integer values of WL ambiguities. Moreover, from the analysis of WLNL, DWL and GF code combinations, we found out that L1 satellite and receiver code hardware delays are large, while E5b and E5a ones rather small. In the third step, we introduce  $N_{25}$  and  $N_{12}$  in a triple frequency phase combination ( $s_{125}$ ) in order to resolve the integer ambiguities  $N_1, N_2, N_5$ . As  $N_{12}$  are only approximated values, the use of TEC values computed by leveling dual frequency phase measurements with GIM allows to fix  $N_{12}$  (and therefore  $N_1, N_2, N_5$ ) at their correct integer values. However, phase hardware delays and antenna phase center delays would cause an error of 2–2.5 TECU through the ambiguity resolution process. In the fourth step, we compute TEC by introducing GF ambiguities  $N_{p,GF}^i$  in either L1/E5b or L1/E5a GF phase combination; E5b/E5a is actually one order of magnitude less precise. Finally, as the error caused by GF phase combination delays on TEC is about 0.2 TECU, the total error on TEC ( $TEC_{12}$  or  $TEC_{15}$ ) would approximately reach 2–3 TECU. The differences between triple frequency TEC values and dual frequency TEC values can be explained by the error budget associated to the GF ambiguity resolution. Unfortunately, as the 2f method is not precise enough, this prevents us to validate our results.

Finally, this method has shown good results but needs further validation, either internal by validation of our theoretical assumptions or external by comparison with other precise TEC values. We could also test it on triple frequency GPS data.

#### Acknowledgments

The GIOVE datasets used for the work presented in this paper have been provided by the European Space Agency. The views presented in the paper represent solely the opinion of the authors and should be considered as research results not strictly related to Galileo Project design. The authors would like to thank the European Space Agency for kindly providing the GIOVE datasets.

## References

- ESA & GSA Galileo Open Service Signal In Space Interface Control Document OS SIS ICD, February 2008.
- Bidaine, B., Warnant, R. Measuring total electron content with GNSS: investigation of two different techniques, in: *Proceeding of the IRST*, Edinburgh, United Kingdom, 2009.
- Brunini, C., Azpilicueta, F. Accuracy assessment of the GPS-based slant total electron content. *J. Geod.* 83 (8), 773–785, 2009.
- Ciraolo, L., Azpilicueta, F., Brunini, C., et al. Calibration errors on experimental slant total electron content (TEC) determined with GPS. *J. Geod.* 81 (2), 111–120, 2007.
- Feltens, J., Schaer, S. IGS products for the ionosphere, in: *Proceeding of the IGS Analysis Center Workshop*, ESA/ESOC, 1998.
- Manucci, A.J., Wilson, B.D., Yuan, D.N., et al. Calibration errors on experimental slant total electron content (TEC) determined with GPS. *Radio Sci.* 33, 565–582, 1998.
- Melbourne, W.G. The case for ranging in GPS-based geodetic systems, in: *Proceeding of the 1st International Symposium on Precise Positioning with the Global Positioning System*, Rockville, Maryland, United States, pp. 373–386, 15–19 April, 1985.
- Orus, R., Hernandez-Pajares, M., Juan, J.M., et al. Performance of different TEC models to provide GPS ionospheric corrections. *J. Atmos. Solar-Terr. Phys.* 64, 2055–2062, 2002.
- Orus, R., Cander, L.R., Hernandez-Pajares, M. Testing regional vertical total electron content maps over Europe during the 17–21 January sudden space weather event. *Radio Sci.* 42 (RS3004), 2007.
- Simsy, A. Three's the charm – triple frequency combinations in future GNSS. *Inside GNSS* 1 (5), 38–41, 2006.
- Simsy, A., Mertens, D., Sleewagen, J.-M., et al. Experimental results for the multipath performance of Galileo signals transmitted by GIOVE-A satellite. *Int. J. Navig. Obs.*, 2008.
- Simsy, A., Sleewagen, J.-M. Performance assessment of Galileo ranging signals transmitted by GSTB-V2 satellites, in: *Proceeding of the ION GNSS*, Forth Worth, United States, 2006.
- Simsy, A., Sleewagen, J.-M., De Wilde, W. et al. Galileo receiver development at Septentrio, in: *Proceeding of the ENC-GNSS*, Munich, Germany, 2005.
- Spits, J., Warnant, R. Total electron content monitoring using triple frequency GNSS data: a three-step approach. *J. Atmos. Solar-Terr. Phys.* 70, 1885–1893, 2008.
- Warnant, R., Pottiaux, E. The increase of the ionospheric activity as measured by GPS. *Earth Planets Space* 52, 1055–1060, 2000.
- Wübbena, G. Software developments for geodetic positioning with GPS using TI 4100 code and carrier measurements, in: *Proceeding of the 1st International Symposium on Precise Positioning with the Global Positioning System*, Rockville, Maryland, United States, pp. 403–412, 15–19 April, 1985.